Phase Structure of Poly(styrene-co-acrylic acid)/Poly(ethylene oxide) Blends by Spin-Label EPR and DSC

Jan Pilar,† Antonin Sikora,† Jiri Labsky,† and Shulamith Schlick*,‡

Institute of Macromolecular Chemistry, Czechoslovak Academy of Sciences, Heyrovsky sq. 2, 162 06 Prague 6, Czechoslovakia, and Department of Chemistry, University of Detroit Mercy, Detroit, Michigan 48219

Received June 5, 1992; Revised Manuscript Received October 6, 1992

ABSTRACT: Blends of poly(styrene-co-acrylic acid) (P(S-AA)) random copolymers with poly(ethylene oxide) (PEO) have been studied by the electron paramagnetic resonance (EPR) spin-label method and by differential scanning calorimetry (DSC). The copolymers contained up to 25 mol % acrylic acid monomers and the blends contained up to 60 wt % PEO. The spin label is attached to some acrylic acid units and provides information on phases containing the copolymer. The presence of *crystalline* PEO in the blends is detected by DSC and verified by wide-angle X-ray scattering (WAXS). EPR and DSC data indicate that pure polystyrene and PEO are immiscible in the temperature range 300-420 K. The presence of *two* amorphous phases is detected by EPR for some blends based on a copolymer containing 5 mol % acrylic acid monomer. The miscibility of the two components in the blend increases with increasing acrylic acid content of the copolymer. The melting points of crystalline PEO have been measured by DSC in untreated blends and in blends annealed by heating above the melting point of pure PEO and crystallization at ambient temperature. The presence of two melting transitions in the annealed samples can be explained by a phase diagram of the system consisting of two amorphous phases with a miscibility gap and a crystalline phase. We suggest that the blend obtained from a solution of the two components is not in thermodynamic equilibrium and emphasize the importance of annealing, especially in systems containing a crystallizable component such as PEO.

Introduction

The existence and extent of phase separation in polymer blends is a problem of great current interest. The detection of a single glass transition temperature T_g is often taken as an indication for complete miscibility of the components in amorphous blends. In some cases however a broad glass transition region is observed, and only spectroscopic methods offer the possibility to detect heterogeneity on a molecular scale.[1]

The spin-labeling method has been applied extensively to the study of motional processes and phase transitions in polymer solutions and in bulk copolymers, polymer blends, and interpenetrating polymer networks.[2-6] Line shapes of EPR spectra from the spin labels, which are stable nitroxide radicals chemically attached to polymers, are sensitive to the rotational mobility of the label in the system. The rotational mobility in turn depends on the temperature, the chemical structure of the polymer, and the solvent viscosity and, in solid samples, on the local composition of the blend and the difference between the sample temperature and the T_g of the system. The separation between outer extrema in the slow-motional EPR spectra of nitroxides ($2A_{zz}'$) can be used to compare *qualitatively* the rotational mobilities of the spin label for various experimental conditions. The rotational mobility can be determined *quantitatively* by comparing experimental and simulated EPR spectra. In some cases the EPR spin label method allows a more detailed description of the heterogeneities in the system, compared to that obtained in DSC studies: For polystyrene/poly(vinyl methyl ether) blends, spin-label studies indicate the presence of *two* distinct environments differing in composition, while DSC measurements indicate only a broad glass transition temperature.[7]

In this report we present a study of blends consisting of PEO and random P(S-AA) copolymers. In this system hydrogen bonding between the carboxylic groups of the comonomer and the ether oxygens in PEO is expected to increase the miscibility of the two components. The difference in the polarity of the two comonomers in P(S-AA) can also supply the thermodynamic drive for miscibility. These two effects have been discussed in a recent study of P(S-AA)/PEO blends, where evidence for hydrogen bonding has been presented.[8]

The present study was motivated by our interest to study the phase structure of the blend on a molecular level, as a function of the acrylic acid content in the copolymer and of the amount of PEO. Analysis of results obtained from three separate techniques (EPR, DSC, and WAXS) provides an opportunity to combine the advantages and to assess the limitations of each method. Important details on the local composition of the blends have been obtained by the study of annealed samples. We suggest that annealing experiments are especially important in blends that contain a crystallizable component.

Experimental Section

Copolymer Synthesis. The monomers styrene and acrylic acid (Fluka) were purified by distillation at 10 Torr under nitrogen. The composition of the monomer mixture is given in Table I. The bulk copolymerization was carried out at 333 K in the presence of 0.15 wt % azobis(isobutyronitrile) (Fluka) to ≈10% conversion. Some acrylic acid units in the copolymer were spin labeled in the second step: The copolymer (3 g) was dissolved in acetone (400 mL), cooled to 278 K, and reacted first at 278 K for 30 min with dicyclohexylcarbodiimide (0.2 g; Fluka) and then at ambient temperature for 2 days with the spin label 4-aminoperdeuterio-2,2,6,6-tetramethylpiperidin-*N*-oxyl.[9] The reaction mixture was concentrated to ≈30 mL; the copolymer was precipitated several times into lightly acidified H_2O (1 mL of 1% H_2SO_4 in 500 mL of H_2O) until the free spin label was not detected by EPR, and dried at 333 K for 3 days at a pressure of 3 Torr. Two types of polymers with no free acid groups were prepared, based on spin labeling of *all* acrylic and methacrylic groups in P(S-AA) and in poly(styrene-co-methacrylic acid) copolymers (P(S-MAA)); these copolymers are in practice spin-labeled polystyrene. The formulas for the spin-labeled polystyrene and copolymers are given in Scheme I.

* Author to whom correspondence should be addressed.
† Czechoslovak Academy of Sciences.
‡ University of Detroit Mercy.

0024-9297/93/2226-0137$04.00/0

Table I
Characterization of P(S–AA) Copolymers[a]

copolymer	V_S (mL)	V_{AA} (mL)	$[AA]_C$ (mol %)	$[AA]_{SLC}$ (mol %)	MW ($\times 10^{-5}$)
P(S–0AA)	20	0.3	5.3	≈0	2.6
P(S–5AA)	20	0.5	7.7	4.8	3.6
P(S–10AA)	30	2.5	13.8	9.5	9.2
P(S–25AA)	30	10.0	34.2	26.3	2.4

[a] V_S and V_{AA} are the amounts of styrene and acrylic acid monomers in the initial polymerization mixture; $[AA]_C$ and $[AA]_{SLC}$ are the concentrations of the acrylic acid in the copolymer and in the spin-labeled copolymer, respectively, determined by titration.

Scheme I

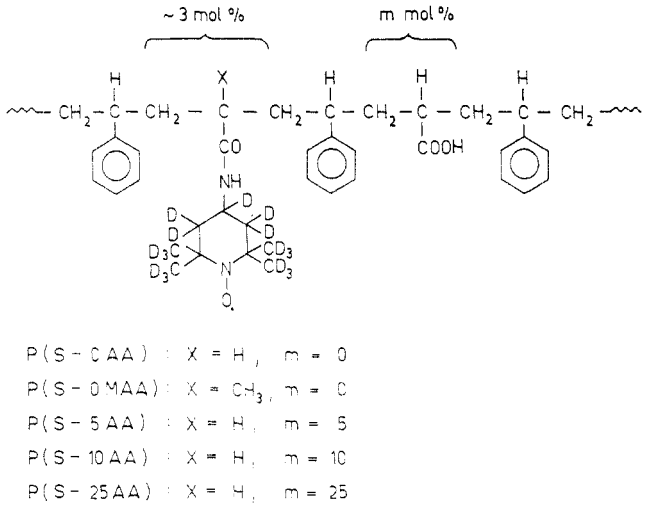

Polymer Characterization. The water content in the copolymer containing the highest amount of acrylic acid units (25 mol %), determined by the Fisher method, was <1 wt %. The concentration of the COOH groups in the copolymers was determined by titration of the polymer solution in a benzene–methanol mixture (9:1 by volume), which also contained a small amount of dioxane, with 0.1 N sodium methoxide in the presence of phenolphthalein. The concentration of the COOH groups in the non-spin-labeled copolymer was in close agreement with the results of elemental analysis.

The mass-average molar mass of the non-spin-labeled copolymers was determined by light scattering in dioxane with a modified Sofica 42.000 instrument at 546 nm and 298 K. The refractive index increments were determined experimentally under the same conditions with a Brice-Phoenix BP-2000 V differential refractometer.

Preparation of Blends. Blends of PEO (MW = 100 000; Aldrich) with the P(S–AA) copolymers were prepared by mixing 2% solutions of the components in benzene–methanol mixtures (9:1 by volume), evaporating in Teflon containers at ambient temperature for 24 h, and drying in vacuum at 333 K for 3 days. The dried blends were stored in a desiccator.

The notation used for the polymer samples is P(S–*m*AA)/*n*PEO, where *m* is the mole percent of free acrylic acid units in the spin-labeled copolymer and *n* is the weight percent of PEO in the blend.

EPR Measurements. X-band EPR spectra were recorded with a Jeol PE-3X spectrometer in Prague and with a Bruker 200D SRC spectrometer in Detroit. All spectra were recorded with a 100-kHz magnetic field modulation at a microwave power of ≤4 mW. The Jeol PE-3X spectrometer was equipped with an EC-100 computer. The sample temperature was stabilized with the JES-VT-3A temperature controller to ±0.5 K and measured with a platinum resistance thermometer. The absolute value of the magnetic field was measured with the MJ-110R Radiopan Poznan NMR magnetometer. The *g* factors were determined relative to the fourth line of Mn^{2+} in a MgO sextet (g = 1.981). The Bruker spectrometer was interfaced with a data acquisition system based on a IBM PC/XT and the software EPRDAS (Mega Systems Solutions, Rochester, NY). The microwave frequency and the absolute value of the magnetic field were measured respectively with the HP 5342A frequency counter and with the Micro-now gaussmeter Model 515B. The *g* factors were determined relative to the signal of Cr^{3+} in MgO (g = 1.9796). In the temperature range 100–420 K EPR spectra were measured with the Bruker 4111VT variable-temperature unit.

Q-band EPR spectra in the temperature range 120–300 K were measured at the National Biomedical ESR Center in Milwaukee, WI, using a spectrometer equipped with a low-noise Gunn diode oscillator.[10]

DSC Measurements. Thermal analysis of the polymers was performed with the DSC-2 Perkin-Elmer calorimeter. The power and temperature were calibrated with a sapphire single crystal of known mass and with indium metal at its melting point, respectively.

Glass transition temperatures T_g in the range 230–450 K were measured with a heating rate of 10 K/min; T_g values were evaluated from the second run.[11] Melting temperatures were measured in the range 290–350 K with a heating rate of 1.25 K/min. The melting points were taken at the maximum of the endotherms, because in some experiments the transition ends were not well-defined. Samples with minimal thermal treatment (heated to 420 K, cooled rapidly to 230 K at a rate of 10 K/min, and measured immediately in the second run) will be designated as "untreated" samples. Some samples were heated for 15 h at 343 K and left to crystallize at ambient temperature for 1 week. These are the "annealed" samples.

WAXS Measurements. These measurements were performed at the Centre d'Études Nucléaires de Grenoble (CENG) in Grenoble, France, using a cobalt source at a wavelength of 1.789 Å. The angular range 2θ was 10–40°.

Simulation of EPR Spectra. Spectra in the slow-motional regime were calculated using the Schneider–Freed set of programs.[12] Lorentzian line shapes and rotationally invariant first derivative peak-to-peak line widths ΔH_{pp} were assumed. A modified version of the Rigid Limit Nitroxide Program was used to simulate rigid limit spectra[13], assuming mixed Gaussian–Lorentzian line shapes and orientationally dependent line widths $\Delta H_{pp}(\phi) = a + b\cos^2\phi$, where ϕ is the polar angle between the *z*-axis in the nitroxide axes system and the direction of the external magnetic field. Corrections to second order in the hyperfine interaction and in the *g*-tensor anisotropy[14] and the $1/g$ correction for field-swept spectra[15] were included in the resonance condition for the allowed EPR transitions. Simulations were performed on a Siemens 7536 computer in Prague and on a HP Vectra RS/20C computer equipped with a 386 processor in Detroit.

Results

In initial experiments we compared the results of thermal analysis for non-spin-labeled polymers with those of the spin-labeled analogues. Because no differences between the two types of polymers was detected, all studies were performed on the spin-labeled polymers.

EPR Spectroscopy. The rigid-limit EPR spectra at 120 K of the spin-labeled copolymers and of all the blends with PEO were essentially identical, except for minor linewidth variations that are assigned to slightly different concentrations of the spin label in the various samples. Similar EPR line shapes have also been detected at 120 K for solid solutions of the spin-labeled copolymers in dimethylformamide (DMF); for mixtures of the copolymers and PEO in DMF; and for spin-labeled polystyrene (P(S–0AA) and P(S–0MAA)) in toluene. The experimental and simulated X-band rigid-limit EPR spectra of solid P(S-5AA) at 120 K are shown in Figure 1a. The simulated spectrum was obtained with the following parameters: A_{xx} = 0.67 mT, A_{yy} = 0.58 mT, A_{zz} = 3.45 mT, g_{xx} = 2.009 35, g_{yy} = 2.005 75, and g_{zz} = 2.001 70. The line width was a combination of Gaussian and Lorentzian line shapes with equal weights. Rigid-limit EPR spectra at Q-band provided an additional check of the **A**- and **g**-tensor components. In Figure 1b we present the experimental Q-band spectrum at 120 K of P(S–0MAA)

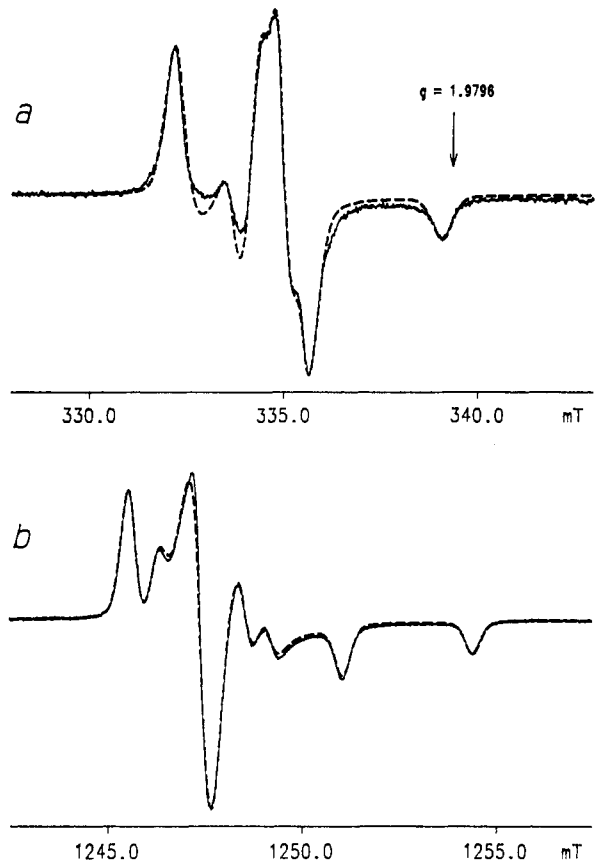

Figure 1. (a) X-band rigid-limit EPR spectrum of the copolymer P(S-5AA) at 120 K (—) and the simulated spectrum (- - -) as described in the text. The parameters for the Gaussian and Lorentzian components of the line shape assuming orientationally dependent line width are $a^G = 0.35$ mT, $b^G = 0.18$ mT, $a^L = 0.23$ mT, and $b^L = 0.13$ mT. (b) Q-band rigid-limit EPR spectrum of the copolymer P(S-0MAA) in toluene solution at 120 K (—) and the simulated spectrum (- - -) as described in the text. The parameters for the Gaussian and Lorentzian components of the line shape assuming orientationally independent line width are $a^G = 0.41$ mT and $a^L = 0.28$ mT.

in toluene and the simulated spectrum calculated with the parameters used at X-band, except $A_{yy} = 0.64$ mT.

The temperature dependence of the X-band EPR spectra of the pure copolymers (no PEO) in the range 340–420 K indicated a *decrease* in the outer extrema separation $2A_{zz}'$ with increasing temperature and an *increase* at higher contents of the acrylic acid monomer at a constant temperature. The $2A_{zz}'$ values are given in Table II.

Addition of up to 60 wt % PEO to P(S-0AA) has no effect on the EPR spectra, even at the high temperatures. Addition of PEO to the copolymer however greatly affects the EPR spectra of the spin label, as seen in the X-band EPR spectra for the copolymer P(S-25AA) at 380 K (Figure 2). The line shapes for 10 and 30 wt % PEO are similar to those for the pure copolymer, but the $2A_{zz}'$ values decrease with increasing PEO content in the blend (Table II). The changes for the blend containing 60 wt % PEO are dramatic and suggest significantly higher mobility of the spin label. The temperature variation of the EPR spectra reinforces the conclusions derived above: A decrease in $2A_{zz}'$ with no significant line shape changes is seen for PEO contents of 10 and 30 wt % with increasing temperature, while for the blend P(S-25AA)/60PEO a motionally narrowed EPR spectrum is obtained.

The EPR spectra given in Figure 2 were simulated using *A*- and *g*-tensor components determined from X-band rigid-limit spectra and a *single set* of rotational diffusion parameters. The simulations are based on the assumption that the spin-label rotational diffusion consists of an approximately isotropic rotational diffusion of the polymer chain segment to which the spin label is bound characterized by the rotational diffusion parameter R_s and an internal rotation of the spin label about the bond to the polymer chain segment characterized by the rotational diffusion parameter R_I. The resulting axially symmetric rotational diffusion of the spin label is therefore characterized by the two components of the rotational tensor $R_\perp = R_S$ and $R_\parallel = R_S + R_I$ and by an angle θ at which the axis of internal rotation, identical with the rotational diffusion symmetry axis, is tilted in the *xz* plane from the *z* axis of the nitroxide axis system. The best fits presented in Figure 2 were obtained for the values of the rotational diffusion tensor components indicated, using jump diffusion as a model of rotational diffusion of the spin label, with $R_j\tau_j = 1$ ($j = \perp, \parallel$) and $\theta \approx 50^0$; τ_j is the mean residence time at each orientation. No significant differences in the segmental motion, and an increase of the *internal* rotational mobility of the spin label with increasing PEO content in the P(S-25AA) blends, were detected (Figure 2).

EPR spectra at 380 K of the blends based on the P(S-5AA) copolymer as a function of PEO content are given in Figure 3. One site for the spin label is detected for the pure copolymer and for the P(S-5AA)/PEO blend containing 10 wt % PEO. EPR spectra of the blends P(S-5MAA)/30PEO and P(S-5AA)60PEO however reveal the presence of *two sites* in all spectra taken above 340 K; this behavior is in contrast to the unique site detected for the P(S-5AA)/10PEO blend and for all blends of the copolymer P(S-25AA), with the possible exception of the P(S-25AA)/60PEO blend (Figure 2). Discrepancies between experimental and simulated spectra suggest a second site for the spin label in the latter blend as well. The complexity of the combined spectra prevents a quantitative analysis. Several qualitative conclusions can however be derived. First, the rotational mobility of the spin labels in the P(S-5AA)/10PEO blend increases with temperature and is higher in the blend compared to that in the pure copolymer; this conclusion follows from the values of the extreme separation (Table II). Second, for a PEO content of 10 wt % the outer extrema separations $2A_{zz}'$ are slightly lower in blends based on a P(S-5AA) copolymer, compared to those based on the P(S-25MAA) copolymer (Table II). Third, we note that the extreme separation of spin labels localized in the less mobile sites observed in the spectra for P(S-5AA)/30PEO and P(S-5AA)/60PEO blends at 380 K are practically the same and only slightly lower than in the P(S-5AA)/10PEO blend (Table II). In addition, the rotational mobility of the spin label in the more mobile site in the P(S-5AA)/60PEO blend is higher, compared to that in the P(S-5MAA)/30PEO blend; this is clearly seen in the spectra presented in Figure 3.

The rotational mobility of the spin label in the P(S-0MAA) copolymer is lower than that in the P(S-AA) copolymer; this has been deduced from the EPR spectra of both bulk copolymers and their solutions in DMF at higher temperatures. This effect is due to the additional methyl group in the comonomer. The absence of line broadening in solutions of the copolymers indicates no contributions from spin–spin interactions and suggests a random copolymer.

Heating of the samples at the high temperatures for the time necessary to obtain the EPR spectra did not result in any changes in the samples, and the spectra were fully reversible in the entire temperature range.

Table II
Temperature Dependence of the Outer Extrema Separation $2A_{zz}'$ (mT) in the Slow-Motional EPR Spectra of Spin-Labeled P(S-AA) Copolymers and P(S-AA)/PEO Blends at Various PEO Contents (Wt %)

	P(S-0AA)	P(S-5AA)				P(S-25AA)			
temp	0	0	10	30	60	0	10	30	60
340 K	6.39	6.47	6.44	6.37	6.37	6.54	6.54	6.50	6.33
380 K	6.30	6.33	6.28	6.20[a]	6.20[a]	6.44	6.37	6.30	5.60[a]
420 K	5.85	6.04	5.90	*b*	*b*	6.32	6.10	5.93	*b*

[a] Data represent the spin labels localized in the less mobile site in the two-site EPR spectra. [b] Motionally narrowed spectra were observed.

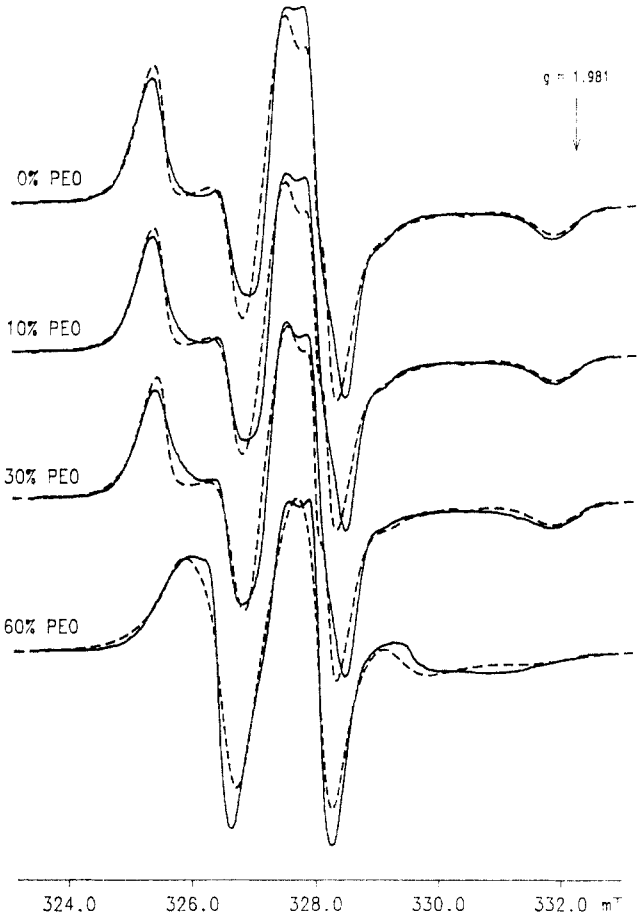

Figure 2. Experimental (—) and simulated (- - -) EPR spectra at 380 K of the copolymer P(S-25AA) and its blends for the indicated PEO contents. All simulated spectra were calculated for jump diffusion with $R_\perp = 1.0 \times 10^6\ s^{-1}$, $\Delta H_{pp} = 0.02$ mT and with $R_\parallel = 1.5 \times 10^8\ s^{-1}$ and $\theta = 47°$ for 0 wt % PEO, $R_\parallel = 1.6 \times 10^8\ s^{-1}$ and $\theta = 47°$ for 10 wt % PEO, $R_\parallel = 1.7 \times 10^8\ s^{-1}$ and $\theta = 47°$ for 30 wt % PEO, $R_\parallel = 3.5 \times 10^8\ s^{-1}$ and $\theta = 55°$ for 60 wt % PEO. Other simulation details are given in the text.

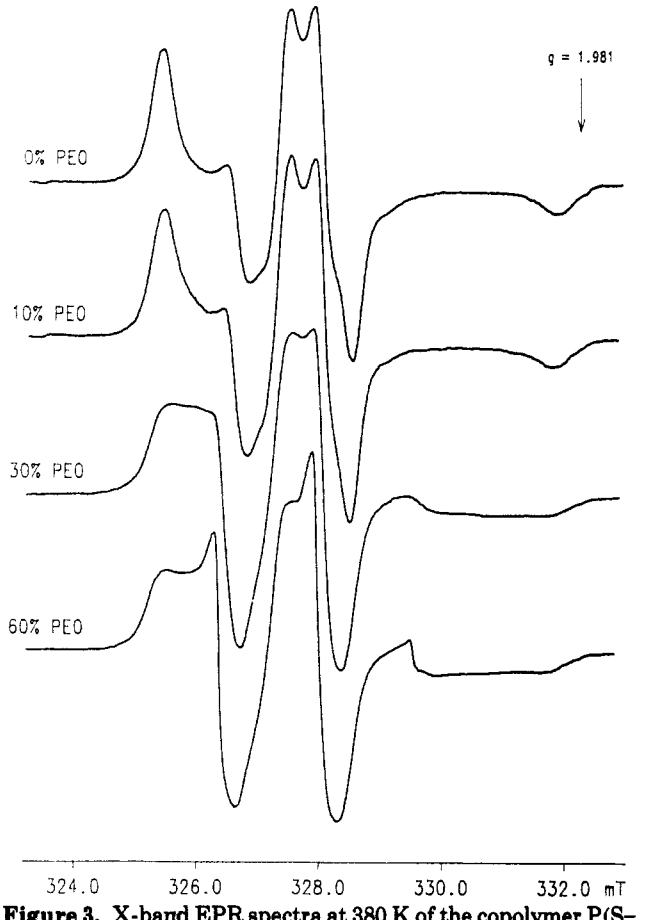

Figure 3. X-band EPR spectra at 380 K of the copolymer P(S-5AA) and its blends for the indicated PEO contents.

DSC Results. The glass transition temperatures T_g of the copolymers and blends are given in Table III, for untreated and annealed samples. We were unable to measure T_g in two cases: in blends based on P(S-5AA) copolymers with more than 10 wt % PEO because of the broad transition region, and in the samples whose glass transitions were covered by a melting endotherm. The T_g values of untreated samples of P(S-25AA) blends with more than 10 wt % PEO were essentially independent of blend composition.

The melting temperatures of PEO crystallites measured in some samples are given in Table IV. Only one melting transition was found in untreated samples. An approximate estimate of the crystalline fraction in the untreated samples can be obtained by using the heat of transition. The amount of PEO in crystalline form in the blends P(S-5AA)/30PEO and P(S-25AA)/30PEO was found to be respectively ≈30% and <2.5%, using the curves presented in Figure 4. These results correlate well with the results of WAXS data, which indicate partial crystallinity of PEO in the P(S-10AA)/30PEO blends and no crystallinity in the P(S-25AA)/30PEO blends.

Table III
Glass Transition Temperatures T_g of P(S-AA) Copolymers and P(S-5AA)/PEO Blends

		T_g (K)	
copolymer	PEO (wt %)	untreated	annealed
P(S-0AA)	0	374.2	
	30	372.8	
	60	376.3	
P(S-5AA)	0	385.1	
	10	333.0	331.8
	20	*a*	*a*
	30	*a*	*a*
	40	*a*	*a*
P(S-25AA)	0	405.1	
	10	355.6	384.2
	20	332.0	326.7
	30	333.0	340.9
	40	329.5	320.7
	60	*b*	*b*

[a] The glass transition region was too broad for accurate reading of the T_g. [b] The glass transition was masked by the melting endotherm.

Table IV
Melting Temperatures of Crystalline PEO in P(S-AA)/PEO Blends

copolymer	PEO (wt %)	untreated T_m (K)	annealed T_{m1} (K)	annealed T_{m2} (K)
P(S-0AA)	30	336.0		333.0
	60	336.0		333.8
	100	337.3		
P(S-5AA)	10		311.4	323.4
	20		311.4	323.3
	30	325.5	315.9	327.3
	40	329.7	316.0	329.9
P(S-25AA)	10			
	20		318.5[a]	
	30		318.0	321.6
	40	331.8	318.0	324.1
	60	329.1	313.4	332.3

[a] No splitting of the melting endotherm was observed.

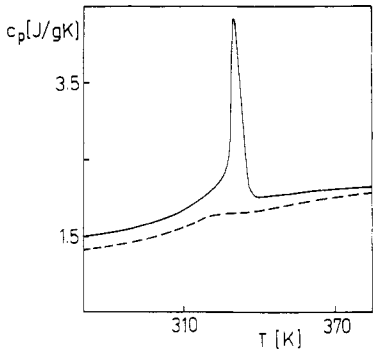

Figure 4. Temperature dependence of the specific heat c_p for the untreated blends P(S-5AA)/30PEO (—) and P(S-25AA)/30PEO (- - -).

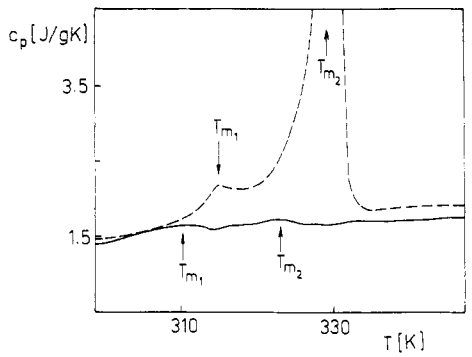

Figure 5. Temperature dependence of the specific heat c_p for the annealed blends P(S-5AA)/20PEO (—) and P(S-5AA)/30PEO (- - -).

Annealing of all P(S-5AA)/PEO and P(S-25AA)/PEO blends containing more than 30 wt % PEO as described above results in the splitting of the melting endotherm into two peaks (Figure 5 and Table IV). The splitting was observed even for a heating rate of 10 K/min.

Discussion

This section is composed of two parts. In the first part we will discuss the results obtained for the untreated samples from EPR spectroscopy and will provide supporting evidence from DSC and WAXS data. In the second part we will suggest a phase diagram for the blends studied, based mainly on an analysis of the melting temperatures measured for the annealed samples by DSC. Finally we will compare our results and conclusions with existing data for this system.

The spin label is attached to the acrylic acid monomer in the copolymer. Therefore the EPR results will reflect the dynamics in the pure copolymer or in domains containing the copolymer and PEO and will not supply direct information on the dynamics of separated PEO.

1. Phase Composition in Copolymers and Untreated P(S-AA)/PEO Blends. As expected only one site for the spin level is detected in spin-labeled P(S-0AA), which is in practice pure polystyrene. Addition of up to 60 wt % PEO to this polystyrene has no effect on the mobility of the spin label, on the glass transition temperature of P(S-0AA), and on the melting temperature of PEO, suggesting a system separated into pure components. This results indicates that without the acrylic acid comonomer the miscibility is negligible, in agreement with previous results.[8]

Incorporation of AA in the copolymer increases slightly the extreme separation in the EPR spectra of pure copolymers in the entire temperature range studied (Table II). This conclusion is in accord with the increase in T_g detected by DSC (Table III).

Two spin label sites were detected in blends of P(S-5AA) with more than 10 wt % PEO (Figure 3), indicating the presence of two amorphous phases containing spin-labeled copolymer, which differ in composition. The broad glass transition region observed in these blends (Table III) confirms this interpretation. The DSC data indicate, in untreated blends based on the P(S-5AA) copolymer, no presence of crystalline PEO for PEO contents of 10 and 20 wt % and a melting PEO endotherm for PEO contents of 30 (Figure 4) and 40 wt %.

In blends based on copolymers with a higher AA content, for example P(S-25AA), EPR data (Figure 2) in the entire range of PEO content 10–60 wt % indicate one dominant environment for the spin label. DSC data for the untreated samples in the range (10–30 wt % PEO indicate no presence of crystalline PEO (Table IV). These results are in agreement with WAXS data mentioned above. All results of the untreated samples indicate therefore the presence of two amorphous phases and a crystalline PEO phase that appears for PEO contents of ≥30 wt % for a low AA content in the copolymer, and the presence of one amorphous phase and a crystalline PEO phase that appears for PEO contents ≥40 wt % for a high AA content in the copolymer.

2. Phase Diagram in P(S-AA)/PEO Blends. Splitting of the melting endotherms into two peaks was detected in all annealed P(S-5AA)/PEO blends. A similar behavior in other systems has been reported and explained in terms of different nucleation mechanisms of crystallization.[16,17] We offer an alternative explanation, in terms of a phase diagram for a binary mixture with a miscibility gap and with one crystalline component,[18] as presented in Figure 6. Unlike the phase diagram used to explain the complex behavior of poly(ε-caprolactone)/polystyrene blends,[19-21] this phase diagram contains the solidus–liquidus curve II in the region of low concentration of the crystallizing component (PEO in our case). The critical point is CP. The two intersection points between the binodal curve and the solidus–liquidus curves I and II (points C and F in Figure 6) determine the monotectic temperature T_M, where two amorphous phases with compositions C and F and a pure crystalline phase are in equilibrium. At T_M a two-component system at constant pressure has no degrees of freedom. Below T_M the composition of the amorphous phase changes along the solidus–liquidus curve II. Metastable parts of the solidus–liquidus curves I and II between the binodal and spinodal curves are represented by lines CD and EF.

Assuming phase equilibrium, the mixture defined by composition K in Figure 6 is expected to separate at an

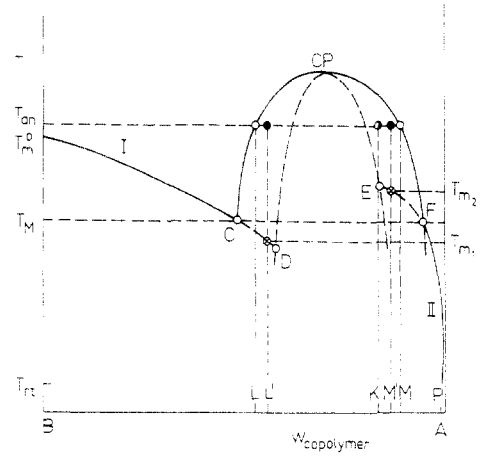

Figure 6. Equilibrium phase diagram of a two-component system with a miscibility gap and one crystalline component. T_m^o is the melting point of the pure crystalline component, T_M is the monotectic temperature, and CP is the critical point.

annealing temperature T_{an} into two equilibrium phases with compositions L and M, respectively. It is very difficult however to reach equilibrium, which is kinetically controlled in polymers. In practice the nonequilibrium time-dependent compositions L′ and M′ are obtained. These compositions are frozen by cooling the sample to ambient temperature T_{rt}. The B component (PEO) crystallizes slowly out of both phases at room temperature. The existence of the two nonequilibrium compositions L′ and M′ in independent domains can result in the formation of two types of crystallites exhibiting different melting temperatures T_{m1} and T_{m2}. The melting temperatures are located at the intersection of ordinates L′ and M′, respectively, with the metastable parts of the solidus–liquidus curves. Therefore the real system under consideration exists in a frozen nonequilibrium state at ambient temperature, and the two melting emdotherms arise from the two types of PEO crystallites, formed from two demixed phases.[22]

The copolymer-rich phase (point M′ in Figure 6) is assumed to dominate in the blends at room temperature. This assumption is supported by the appearance of PEO crystallites with the higher melting temperature T_{m2} that crystallize from this phase in the untreated blends P(S–5AA)/30PEO and P(S–5AA)40PEO (Table IV), and by the higher population of the spin label in the less mobile sites detected in the EPR spectra for these blends (Figure 3). Separation continues during prolonged annealing and results in the formation of PEO crystallites with lower melting temperature T_{m1}, which appear from the minor phase richer in PEO. Detection of the two melting endotherms in annealed P(S–5AA)/10PEO and P(S–5AA)/20PEO blends (Table IV) suggests a limited miscibility of P(S–5AA) copolymers even with a small amount of PEO. The EPR spin-label method cannot identify the two sites in the P(S–5AA)/10PEO blend, most probably because of the small amount of the PEO-rich phase.

The relatively narrow glass transition region observed for the P(S–25AA) copolymer blends with PEO contents of 10–40 wt % (Table III), the absence of PEO melting endotherms in untreated blends of this copolymer with PEO contents of 10–30 wt % (Table IV), and the single site detected in the EPR spectra of these blends (Figure 2) suggest the presence of a dominating homogeneous amorphous phase in the blends based on the copolymer P(S–25AA) with low amounts of PEO. The conclusion is supported by the WAXS data. However, detection of the PEO melting endotherm in the annealed P(S–25AA)/20PEO blend, the splitting of the melting endotherms observed in the annealed blends with this copolymer containing 30–60 wt % PEO (Table IV), and the detection by EPR of a small amount of a second site in the P(S–25AA)/60PEO blend point to the presence of a second amorphous phase in the blends based on this copolymer and containing more than 20 wt % PEO. We suggest that complete miscibility of the P(S–25AA) copolymer with PEO leading to one amorphous phase in the blend is limited to blends containing not more than 10 wt % PEO.

The obvious conclusion from this discussion is the formation of two types of crystallites with different melting temperatures in binary polymer mixtures with one crystallizing component and with a miscibility gap. Limited miscibility of both P(S–5AA) and P(S–25AA) copolymers with PEO is also suggested by the experimental data presented in this study. The two T_g values determined in the blends of the P(S–12AA) copolymer with PEO[23] confirm this conclusion. Comparison of the rotational mobility of the spin label localized in less mobile sites in P(S–5AA)/30PEO and P(S–5AA)/60PEO blends with that in the P(S–5AA)/10PEO blend suggests location of the binodal curve in the region of high copolymer content to the vicinity of 90 wt % copolymer in the P(S–5AA) copolymer blends with PEO and its shift to the higher PEO concentration in blends with the P(S–25AA) copolymer. This conclusion is supported by the higher rotational mobility of the spin label in the less mobile sites in the blends containing P(S–25AA), compared with the blends containing P(S–5AA).

Comparison of the DSC results presented in this study with those in the literature indicates the complexity of the phase behavior in this system and points to the need for, and importance of, annealing of blends for extended periods of time, in order to understand the phase diagram and the effect of the blend composition on the morphology and annealing behavior. Additional studies of blends with specific interactions[24] between the components will be investigated.

Conclusions

Blends of poly(styrene-*co*-acrylic acid) (P(S–AA)) random copolymers with poly(ethylene oxide) (PEO) have been studied by the EPR spin-label method and by DSC. The copolymers contained up to 25 mol % acrylic acid and the blends contained up to 60 wt % PEO. EPR and DSC data indicate that pure polystyrene and PEO are immiscible in the temperature range 300–420 K. The presence of two amorphous phases was detected by EPR for blends based on the P(S–5AA) copolymer containing more than 10 wt % PEO. The miscibility of the two components in the blend increases with increasing acrylic acid content of the copolymer. The detection of two melting transitions by DSC in the annealed blends can be explained by a phase diagram of the binary mixture with a miscibility gap and a separate crystalline phase. The complete miscibility of the P(S–25AA) copolymer with PEO and the presence of only one amorphous phase in the blend seem to be limited to blends containing not more than 10 wt % PEO. We suggest that the blend obtained from a solution of the two components is not in thermodynamic equilibrium and emphasize the importance of obtaining data for annealed samples, especially in systems containing a crystallizable component.

Acknowledgment. This research was supported by Czechoslovak Academy of Sciences Grant Nos. 45023 and 45012. J.P. is grateful for support in Detroit by National

Science Foundation Grant DMR-8718947 (Polymers Program) and by Army Research Office Grant DAA03-86-G-0059. The Q-band experiments at the National Biomedical ESR Center in Milwaukee, WI, were supported by NIH Grant RR-01008. We thank Christofer C. Felix for his assistance with these experiments, Dr. Gerard Gebel of CENG–Grenoble for the WAXS measurements, Dr. J. Stejskal for MW determinations, and E. Palchetkova and D. Kotikova of the Prague IMC for analytical measurements. S.S. is grateful for the hospitality of the IMC in Prague and for the 1991/92 Founders' Fellowship of the American Association of University Women (AAUW).

References and Notes

(1) Yang, H.; Hadziioannou, G.; Stein, R. S. *J. Polym. Sci., Polym. Phys. Ed.* **1983**, *21*, 159.
(2) Pilar, J.; Labsky, J. *J. Phys. Chem.* **1986**, *90*, 6038.
(3) Pilar, J.; Labsky, J. *Macromolecules* **1991**, *24*, 4188.
(4) Schlick, S.; Harvey, R. H.; Alonso-Amigo, M. G.; Klempner, D. *Macromolecules* **1989**, *22*, 822.
(5) Shimada, S.; Kashima, K.; Hori, Y.; Kashiwabara, H. *Macromolecules* **1990**, *23*, 3769.
(6) Chen, W. P.; Schlick, S. *Polymer* **1990**, *31*, 308.
(7) Muller, G.; Stadler, R.; Schlick, S. *Makromol. Chem. Rapid Commun.* **1992**, *13*, 117.
(8) Jo, W. H.; Lee, S. C. *Macromolecules* **1990**, *23*, 2261.
(9) Labsky, J.; Pilar, J.; Lovy, J. *J. Magn. Reson.* **1980**, *37*, 515.
(10) Strangeway, R. A.; Ishii, T. K.; Hyde, J. S. *IEEE Trans. Microwave Theory Tech.* **1988**, *36*, 792.
(11) Richardson, M. J.; Savill, N. G. *Polymer* **1975**, *16*, 753.
(12) Schneider, D. J.; Freed, J. H. In *Biological Magnetic Resonance*; Berliner, L. J., Reuben, J., Eds.; Plenum Press: New York, 1989; Vol. 8, p 1.
(13) Polnaszek, C. F. Ph.D. Dissertation, Cornell University, Ithaca, NY, 1974.
(14) Taylor, P. C.; Baugher, J. F.; Kriz, H. M. *Chem. Rev.* **1975**, *75*, 203.
(15) Aasa, R.; Vanngard, T. *J. Magn. Reson.* **1975**, *19*, 308.
(16) Frensch, H.; Jungnickel, B.-J. *Colloid Polym. Sci.* **1989**, *267*, 16.
(17) Godowsky, Y. K.; Yanul, N. A.; Bessonova, N. P. *J. Colloid Polym. Sci.* **1991**, *269*, 901.
(18) Haase, R.; Schonert, H. *Solid–Liquid Equilibrium*; Pergamon Press: New York, 1969.
(19) Tanaka, H.; Nishi, T. *Phys. Rev. Lett.* **1985**, *55*, 1102.
(20) Tanaka, H.; Nishi, T. *Phys. Rev. A* **1989**, *39*, 783.
(21) Li, Y.; Stein, M.; Jungnickel, B.-J. *Colloid Polym. Sci.* **1991**, *269*, 772.
(22) Wunderlich, B. *Macromolecular Physics*; Academic Press: New York, 1976; Vol. 2.
(23) Jo, W. H.; Kwon, Y. K.; Kwon, I. H. *Macromolecules* **1991**, *24*, 4708.
(24) Tevari, N.; Srivastava, A. K. *Macromolecules* **1992**, *25*, 1013.